

Spatial Resolution of EEG Source Reconstruction in Assessing Brain Connectivity Analysis

Jorge Ivan Padilla-Buriticá^{1,2}(✉), J.D. Martínez-Vargas¹, A. Suárez-Ruiz¹,
J.M. Ferrandez², and G. Castellanos-Dominguez¹

¹ Universidad Nacional de Colombia, Manizales, Colombia
jipadilla@unal.edu.co

² Universidad Politécnica de Cartagena, Cartagena, Spain

Abstract. Brain connectivity analysis has emerged as a tool to associate activity generated in diverse brain areas, making possible the integration of functionally specialized brain regions in networks. However, estimation of the areas with relevant activity is well influenced by the applied brain mapping methods. This paper carries out the comparison of three reconstruction principles that differ in the way the prior covariance is adjusted, including its generalization through multiple and sparse spatial priors. To cluster the locations with significant brain activity (regions of interest), we select the most powerful areas, for which the functional connectivity is measured by the coherence and Kullback-Liebler divergence. From the obtained results on simulated and real-world EEG data, both measures show that the mapping method that includes Multiple Sparse Priors allows improving the connectivity accuracy regardless the used measure for all tested values of added noise.

1 Introduction

In the last years, connectivity analysis has gained considerable importance to study the behavior of the brain during different tasks and cognitive processes, as well as in the detection of some pathological conditions. In this regard, several approaches have discussed whether the connectivity analysis should be performed on EEG channel space or source space. As a result, it has been shown that due to the effects of field spread, it is difficult to carry out a connectivity analysis in the measured recordings on the scalp [15]. Moreover, it is difficult to associate an anatomical meaning with the connections, as the measured signals do not locate in direct spatial proximity to the underlying sources. On the other hand, EEG reconstruction methods (each time achieve better performance on space and time domains), because they take into account the propagation of cortical activity towards the scalp. Furthermore, when the connectivity analysis is performed at the source level, it might yield a better interpretation of calculated interactions, which can be easily associated with the brain processes of integration and segregation [14].

Unfortunately, despite the latest advances in source connectivity analysis, several problems that directly influence the accurateness of this analysis have not been solved. These problems can be summarized as: (i) developing a realistic conductivity model of the head, (ii) selection of the brain mapping method, (iii) selection of a proper connectivity measure and (iv) validation of the obtained results. In this work, we focus in how the chosen brain mapping method influences the performance of the source connectivity analysis.

In this regard, to select the brain mapping method, it must be considered that there exist several models to estimate the source activity, which can be classified into two groups: (i) dipole-fitting models that represent brain activity as a small number of dipoles with unknown positions and, (ii) the distributed-source models that represent the brain activity as a large number of dipoles in fixed positions [5]. Distributed source models present a highly ill-posed inverse problem, with no unique solution in the most general unconstrained case. Consequently, a unique solution can only be obtained by making additional assumptions (spatial and temporal) about the neural activity. For example, these assumptions can be made by introducing prior beliefs on the structure of possible source configurations in Bayesian inference framework [11] or based on geometric or physiological properties of the brain. In this regard, the more realistic the considered assumptions, the more accurate the reconstructed source space, and consequently, the connectivity analysis. However, to the best of our knowledge, there are no studies that systematically consider the influence of estimated source activity over the source connectivity analysis, in spite of the fact that brain mapping errors are known to have a significant effect on the accuracy of connectivity [4].

In this work, we compare three methods solving the inverse problem due to they have a common mathematical framework differing only in the prior assumptions of the estimation of the source covariance matrix. This prior covariance adjusts the primary differences between often used regularization schemes in the source estimation and is generalized by the use of multiple and sparse spatial priors. The comparison approach comprises three stages: (i) brain activity is estimated through Empirical Bayesian Beamformer (BMF) [1], Low-resolution brain electromagnetic tomography (LORETA) [13] and Multiple sparse priors (MSP) [6] approaches. (ii) Some regions of interest are selected based on the recovered sources with the highest energy. (iii) A connectivity brain measure is employed to quantify the changes in the information flow over the selected regions of interest. Obtained results show that the performance of brain connectivity depends strongly on the employed mapping method because different regions of interest (ROI) are obtained and, in the lower degree, on the used measure of similarity between the estimated regions of interest.

2 Methods

2.1 Estimation of Brain Source Activity

With the aim of estimating brain activity from measured EGG recordings, We will consider the following distributed inverse solution $\mathbf{Y} = \mathbf{L}\mathbf{J} + \boldsymbol{\Xi}$, so that

$\mathbf{Y} \in \mathbb{R}^{C \times T}$ is the EEG data measured by $C \in \mathbb{N}$ sensors at $T \in \mathbb{N}$ time samples, $\mathbf{J} \in \mathbb{R}^{D \times T}$ is the amplitude of the $D \in \mathbb{N}$ current dipoles, which placed in each three-dimensional dimension and distributed through cortical surface, and the lead field matrix $\mathbf{L} \in \mathbb{R}^{C \times D}$ is the relationship between sources and EEG data. Besides, the EEG measurements are assumed to be corrupted by zero mean Gaussian noise $\boldsymbol{\Xi} \in \mathbb{R}^{C \times T}$, having matrix covariance $\mathbf{Q}_{\boldsymbol{\Xi}} = \sigma_{\boldsymbol{\Xi}}^2 \mathbf{I}_C$, where $\mathbf{I}_C \in \mathbb{R}^{C \times C}$ is an identity matrix, and $\sigma_{\boldsymbol{\Xi}}^2$ is the noise variance. Under these constraints, brain source activity can be estimated as:

$$\hat{\mathbf{J}} = \mathbf{Q}\mathbf{L}^\top(\mathbf{Q}_{\boldsymbol{\Xi}} + \mathbf{L}\mathbf{Q}\mathbf{L}^\top)^{-1}\mathbf{Y}, \quad (1)$$

being $\mathbf{Q} \in \mathbb{R}^{D \times D}$ the source covariance matrix. For EEG brain mapping, the used approaches differ in the imposed prior assumptions upon \mathbf{Q} as follows:

- *Low-Resolution Brain Electromagnetic Tomography* (LORETA) or maximally smoothed solution, $\mathbf{Q} = \mathbf{I}_D$.
- *Empirical Bayesian Beamformer* (BMF) that imposes spatial priors to include multiple modalities and subjects. In practice, the global prior assumes a covariance with the following q_{dd} element of the main diagonal:

$$q_{dd} = (\mathbf{l}_d^\top(\mathbf{Y}\mathbf{Y}^\top)\mathbf{l}_d)^{-1}/\delta_d, \quad \forall d = 1, \dots, D,$$

where $\mathbf{l}_d \in \mathbb{R}^{C \times 1}$ stands for the d -th column of \mathbf{L} , and $\delta_d = 1/\mathbf{l}_d^\top\mathbf{l}_d$ is the normalization parameter. So, the source covariance is $\lambda_p\mathbf{Q}$.

- *Multiple Sparse Priors* (MSP) that constructs the source covariance as a weighted sum of P possible patches $\{\mathbf{Q}_p; p \in P\}$ so that each one regards a single potentially activated cortex region and is weighted by its respective hyperparameter, $\lambda_p \in \mathbb{R}^+$, as follows:

$$\mathbf{Q} = \sum_{p \in P} \exp(\lambda_p)\mathbf{Q}_p.$$

2.2 Measurement of Brain Connectivity

To assess the brain connectivity analysis, we calculate, within the distributed brain networks, a set of relevant regions of interest (ROI) that make evident the existence of meaningful brain neural activity for the task at hand. Therefore, we must localize a set of reproducible and accurate cortical ROIs that should be consistent for all tested subjects. From EEG data, each brain is parcelled into a set of ROI by selecting those areas encircling the recovered sources with the highest energy. Each ROI area of the cortical surface has a 10 mm radius, covering approximately 300 dipoles, as suggested in [3]. However, the close active dipoles are gathered so that each one belongs to just one ROI, avoiding spurious connectivity. Further, the averaged time series over each ROI is extracted to analyze the functional connectivity among all obtained regions. Thus, we estimate the functional connectivity for the computed ROI sets, using the following measures:

- *Coherence*: This real-valued bivariate measure of the correlation between signals $u(t)$ and $v(t)$ is defined through their spectral representations, $S_{u,v}(t, f)$ [8]:

$$\rho_{uv}(t, f) = \frac{\langle S_u(t, f)S_v^*(t, f) \rangle}{\langle |S_u(t, f)| \rangle \cdot \langle |S_v(t, f)| \rangle} \quad (2)$$

- *Kullback-Liebler (K-L) divergence* that is computed for the random processes \mathbf{u} and \mathbf{v} with finite states u_i and v_i , respectively, as follows:

$$\varrho(\mathbf{u}, \mathbf{v}) = H(\mathbf{u}, \mathbf{v}) - H(\mathbf{u}), \quad \varrho(\mathbf{u}, \mathbf{v}) \in \mathbb{R}^+ \quad (3)$$

where $H(\mathbf{u}) = -\sum_{n \in N} p(u_n) \log p(u_n)$ is the entropy of \mathbf{u} and $H(\mathbf{u}, \mathbf{v}) = -\sum_{n \in N} p(u_n, v_n) \log p(u_n, v_n)$ is the cross entropy between \mathbf{u} and \mathbf{v} .

3 Experimental Set-Up and Results

For the purpose of validation, we investigate the influence of neural reconstruction on the brain connectivity analysis calculated from the assessed ROI sets. Due to the shared mathematical framework, we compare three inverse problem solutions (LORETA, BMF, MSP), differing only in the prior assumptions made upon the estimation of source covariance.

Simulated EEG Data. Initially, we simulate the EEG data that reproduce different brain activities. To this end, two active dipoles are assumed, where each one is a nonstationary source. All non-stationary time series are generated using the real Morlet wavelet, encouraging a behavior similar to an evoked response potential. Each recording lasts 1.5 s length and is sampled at 200 Hz. The random central frequency of the Morlet wavelet is sampled from a Gaussian distribution with a mean 9 Hz and standard deviation 2 Hz. The produced stimulus starts at $t=0$ and the activity is propagated from simulated active dipole #1 to #2 at $t=0.1$ s. Besides, the background noise of the dipole signals is set to have a $1/f$ spectral behavior. Then, each simulated EEG is calculated by multiplying the simulated brain activity to the lead field matrix. For source space modeling, a tessellated surface of the gray-white matter interface is used that has 8196 vertices (possible source localizations) with source orientations fixed orthogonally to the surface. Also, the lead fields are computed by the BEM volume conductor with a mean distance between neighboring vertices adjusted to 5 mm. As a result, we obtain synthetic EEG data for 128-channels. Three experimental configurations, carrying out 100 simulations each one, are performed to test sensibility to the noise of the proposed connectivity-based approach. To this, measurement noise is added to obtain SNR levels, ranging from -6 till 6 dB. Location of active dipoles is randomly selected for each simulation.

Real-World EEG Database. We also carry out the experimental testing using an EEG database provided by the *Wellcome Trust Centre for Neuroimaging*, holding faces and scrambled faces. This data were collected from a single

subjects at the time he made symmetry judgements on faces and scrambled faces as described in [10]. All EEG recordings were acquired on a 128-channel ActiveTwo system, sampled at 2048 Hz, plus electrodes on left earlobe, right earlobe, and two bipolar channels. The epochs (168 faces and 168 scrambled faces) were baseline-corrected from 200 to 0 ms. Also, data were down-sampled at 200 Hz and averaged for each condition. For modeling the source space, we used a tessellated surface of the gray-white matter interface with 8196 vertices (possible source localizations) with source orientations fixed and being orthogonal to the surface. Finally, the head model was computed using a boundary element method (BEM) to estimate the forward operator \mathbf{L} .

Validation Results of Simulated EEG Data. Figure 1 shows the values of connectivity computed between each couple of the simulated sources depending on the employed estimator of neural activity. The connectivity values of a couple of sources are estimated after carrying 100 runs, allocating randomly over the head surface either source for each trial. As expected, the coherence measure (plotted by dashed lines) rises as the SNR level grows higher. By contrast, the K-L divergence (plotted in continued lines) reduces as the noise level decreases. At the same time, the assessed connectivity measures are differently influenced by the used mapping approach. Thus, the use of MSP makes either connectivity measure to be more accurately estimated regardless of the SNR added.

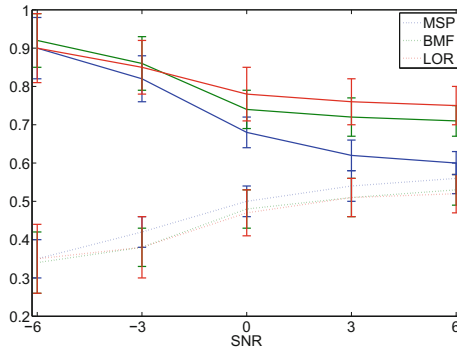


Fig. 1. Assessed values of connectivity after using different mapping approaches: coherence (dashed lines), KL divergence (continuous lines)

It is worth noting that either used estimator of connectivity shows very close standard deviation (KL-divergence provides 0.054 while coherence -0.058), making both measures similar in terms of confidence.

Validation Results of ERP Data. Figure 2 shows the estimated ROIS after mapping as well as the obtained values of connectivity (matrix of coherence). For either testing paradigm (termed *faces* or *scrambled faces*), the top row

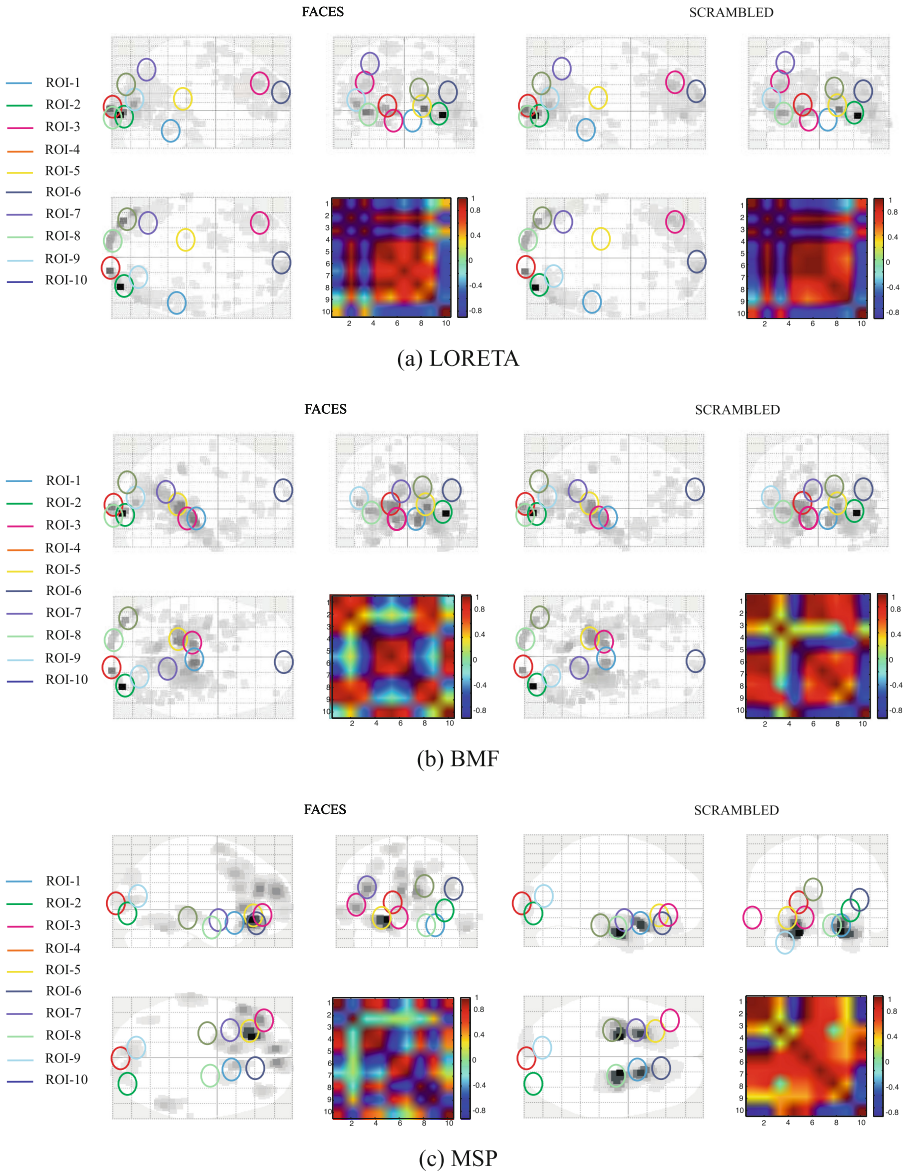


Fig. 2. EEG brain activity estimated by each considered brain mapping approach for a concrete task with the paradigm *faces* and *scrambled faces*. (Color figure online)

(see Fig. 2a) shows the lateral, superior, and sagittal views of the performed LORETA mapping, where the estimated ROIs are marked by circles with a different color. Likewise, Fig. 2b and c display performed results for the BMF and MSP methods, respectively. Visual inspection allows concluding that every tested

mapping registers activity in the visual cortex (Occipital Lobe) and somatosensory area. So far, this finding totally agrees the commonly accepted physiological interpretation about visual stimulation. However, each mapping approach produces different amounts of spurious activity that is identified as ROI, but without any reported clinical meaning. Thus, LORETA provides the highest number of meaningless connections as can be corroborated in the coherence matrix, yielding an activity in areas where it is assumed not to be at all, namely, ROI 3 (Broca's area), ROI 5 (Motor function), ROI 7 (Wernicke's area). This result may be explained because of its widely-known poor spatial resolution. Further, BMF performs fewer ROIs with spurious, having even the less power. So, Broca's and Wernicke's (rather related to speech) areas, Motor function and auditory areas are wrongly labeled as salient ROIs for face recognition. Lastly, MSP produces lower values of coherence for ROIs not belonging to the occipital lobe. As a result, MSP yields the lowest number of the wrong ROIs, and thus, it promotes the most accurate connectivity estimation since it focuses most of the estimated ROIS on the Occipital lobe (ROI 4), linking correctly to the visual area.

For either paradigm *faces* (Top row) and *scrambled faces* (bottom row), Fig. 3 displays the values of connectivity computed by the K-L divergence upon the same ROI set as in the case of the coherence measure. Although every mapping method produces the same groups of associated activity, the MSP method makes more evident the relation among ROIs (see Fig. 3c and f).

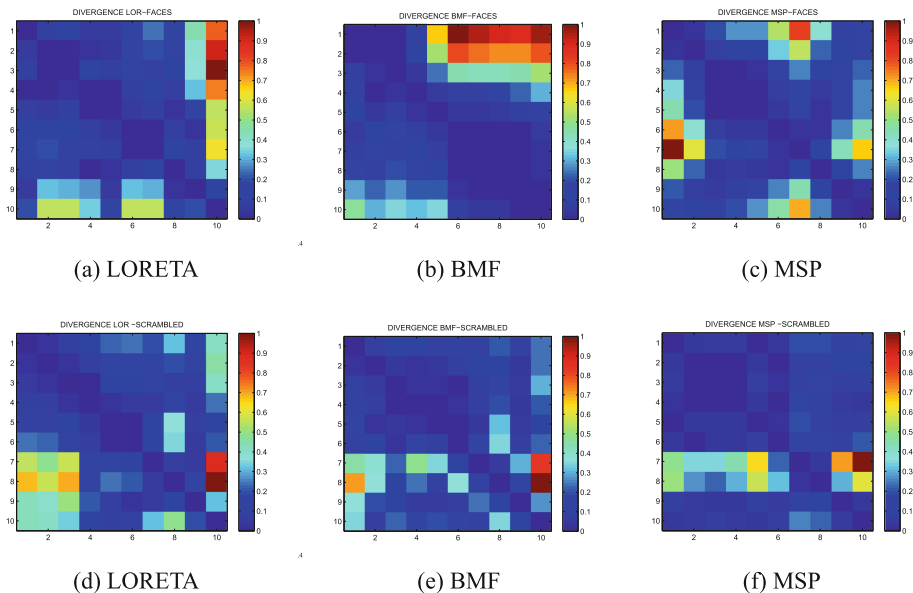


Fig. 3. Estimated matrices of connectivity using the K-L divergence for either paradigm *faces* (Top row) and *scrambled faces* (bottom row).

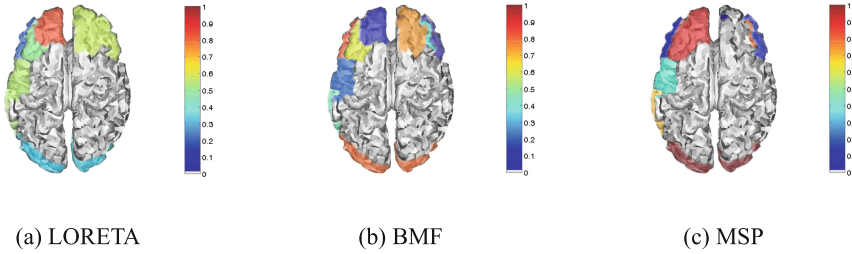


Fig. 4. Results of the paired t -test for the estimated sets of ROI by each mapping method with K-L divergence.

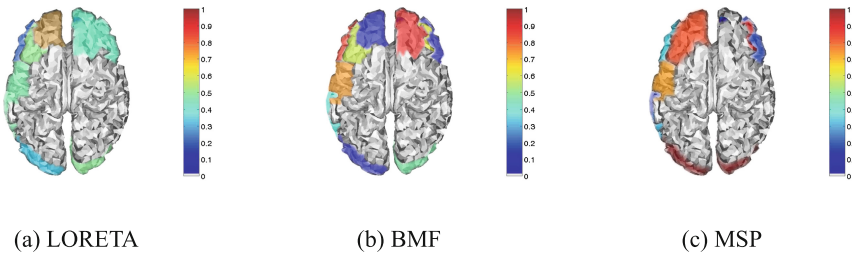


Fig. 5. Results of the paired t -test for the estimated sets of ROI by each mapping method with Coherence.

On the other hand, we carry out the paired t -test over the set of estimated ROIs to make clear which areas contribute the most to differentiate between the different conditions, namely, faces and scrambled faces. For the sake of generalization, we also merge the obtained sets of ROI for both considered paradigms. As a result, the most discriminating areas are identified in the occipitotemporal brain (see Figs. 4 and 5). Meanwhile, this area has been reported to be related to the structural encoding of faces [12]. In this regard, MSP is the mapping technique that shows the most powerful and localized activity in the occipitotemporal area, favoring the interpretation of the assessed connectivity measures.

4 Discussion and Concluding Remarks

We have investigated the influence of EEG source reconstruction for brain connectivity analysis, according to the following steps:

1. Selection of brain mapping method, contrasting LORETA, BMF and MSP
2. ROI selection based on the estimated maps of neural activity
3. We apply two connectivity measures: Kullback-Leibler divergence and Coherence

The main aspect concerns the selected brain mapping method for imaging EEG activity. The first tested method of brain mapping was LORETA has a relatively low spatial resolution because the localization is preserved with a certain amount of dispersion [13]. Therefore, the estimated brain activity is more blurred, producing broad zones of neural activity. On the other hand, the use of BMF improves identification of the source signals from electroencephalographic measurements [1], nevertheless, BMF tends to estimate several spurious activated areas, misleading the connectivity analysis. This effect appears to be directly related to the estimation complexity of the source covariance matrix [12].

On the other hand, MSP allows to perform source activity reconstruction so that we obtain more precise regions of activation. Furthermore, due to the low spatial resolution, LORETA algorithm often locates erroneous regions with activity, where powerful common sources should not be present. Therefore, although LORETA has been widely used in the last years to reconstruct brain activity, its confidence of estimated areas of activation may be not enough [7]. From obtained results validating on simulated and real-world recordings, MSP-based estimation of ROI time courses allows improving the connectivity accuracy regardless the used measure for all tested values of SNR. Furthermore, MSP allows estimating ROIs centered at locations related to the experimental task at hand (i.e., face perception). Thus, the estimated energy has greater activity in the visual cortex (Occipital Lobe) and the somatosensory area for either testing paradigm (faces or scrambled faces). This result totally matches the accepted physiological interpretation about visual stimulation.

Generally speaking, a challenging issue relating to brain connectivity analysis is how to identify ROI sets (obtained from the brain mapping method) precisely, at very short temporal scales; this dilemma remains common for all cognitive tasks [9] and for the study of the brain pathologies [2, 16]. We have used an approach to select regions of interest ROI similar to [12], in order to ensure that the selected regions of interest have been the ones that have had the most energy and best describe the behavior of brain states. As a result, the introduced ROI sets enhance the performed detection accuracy. Another aspect of consideration is the involved measure of connectivity analysis. Here, we compare both Kullback-Liebler divergence and Coherence measures that provide similar behaviors as already had been reported in the literature [8]. Nevertheless, the used EEG source estimation method clearly influences the assessed connectivity. For instance, a poor source reconstruction may lead the incorrect selection of ROIs for separating responses to different stimulus. As a result, the source estimation method must be chosen carefully in all studies conducted in brain connectivity. As future work, authors plan to test the introduced approach over diverse paradigms, clustering, and connectivity measures. Furthermore, an online extension of the brain connectivity analysis can be proposed to include the temporal variations of the inter-channel relationships directly.

Acknowledgments. This work was supported by the research project 11974454838 funded by COLCIENCIAS. J.I. Padilla-Buriticá is founded by Programa nacional de becas de doctorado, convocatoria 647 (2014).

References

1. Belardinelli, P., Ortiz, E., Barnes, G., Noppeney, U., Preissl, H.: Source reconstruction accuracy of MEG and EEG Bayesian inversion approaches. *PLoS ONE* **7**(12), 51985 (2012)
2. Brier, M.R., Thomas, J.B., Fagan, A.M., Hassenstab, J., Holtzman, D.M., Benzinger, T.L., Morris, J.C., Ances, B.M.: Functional connectivity and graph theory in preclinical Alzheimer's disease. *Neurobiol. Aging* **35**(4), 757–768 (2014)
3. Brookes, M.J., O'Neill, G.C., Hall, E.L., Woolrich, M.W., Baker, A., Palazzo Corner, S., Robson, S.E., Morris, P.G., Barnes, G.R.: Measuring temporal, spectral and spatial changes in electrophysiological brain network connectivity. *NeuroImage* **91**, 282–299 (2014)
4. Cho, J.-H., Vorwerk, J., Wolters, C.H., Knösche, T.R.: Influence of the head model on EEG and MEG source connectivity analyses. *Neuroimage* **110**, 60–77 (2015)
5. Costa, F., Batatia, H., Oberlin, T., D'Giano, C., Tourneret, J.-Y.: Bayesian EEG source localization using a structured sparsity prior. *NeuroImage* **144**, 142–152 (2017)
6. Friston, K., Harrison, L., Daunizeau, J., Kiebel, S., Phillips, C., Trujillo-Barreto, N., Henson, R., Flandin, G., Mattout, J.: Multiple sparse priors for the M/EEG inverse problem. *NeuroImage* **39**(3), 1104–1120 (2008)
7. Grech, R., Cassar, T., Muscat, J., Camilleri, K.P., Fabri, S.G., Zervakis, M., Xanthopoulos, P., Sakkalis, V., Vanrumste, B.: Review on solving the inverse problem in EEG source analysis. *J. Neuroeng. Rehabil.* **5**(1), 25 (2008)
8. Greenblatt, R.E., Pflieger, M.E., Ossadtchi, A.E.: Connectivity measures applied to human brain electrophysiological data. *J. Neurosci. Methods* **207**(1), 1–16 (2012)
9. Hassan, M., Dufor, O., Merlet, I., Berrou, C., Wendling, F.: EEG source connectivity analysis: from dense array recordings to brain networks. *PLoS One* **9**(8), 105041 (2014)
10. Henson, R.N., Wakeman, D.G., Litvak, V., Friston, K.J.: A parametric empirical Bayesian framework for the EEG/MEG inverse problem: generative models for multi-subject and multi-modal integration. *Front. Hum. Neurosci.* **5**, 76 (2011)
11. Nummenmaa, A., Auranen, T., Hämäläinen, M.S., Jääskeläinen, I.P., Lampinen, J., Sams, M., Vehtari, A.: Hierarchical Bayesian estimates of distributed MEG sources: theoretical aspects and comparison of variational and MCMC methods. *NeuroImage* **35**(2), 669–685 (2007)
12. Padilla-Buriticá, J.I., Martínez-Vargas, J.D., Castellanos-Dominguez, G.: Emotion discrimination using spatially compact regions of interest extracted from imaging EEG activity. *Front. Comput. Neurosci.* **10** (2016)
13. Pascual-Marqui, R.D., Esslen, M., Kochi, K., Lehmann, D., et al.: Functional imaging with low-resolution brain electromagnetic tomography (LORETA): a review. *Methods Find. Exp. Clin. Pharmacol.* **24**(Suppl C), 91–95 (2002)
14. Rubinov, M., Sporns, O.: Complex network measures of brain connectivity: uses and interpretations. *Neuroimage* **52**(3), 1059–1069 (2010)
15. Schoffelen, J.-M., Gross, J.: Source connectivity analysis with MEG and EEG. *Hum. Brain Mapp.* **30**(6), 1857–1865 (2009)
16. Sheline, Y.I., Raichle, M.E.: Resting state functional connectivity in preclinical Alzheimer's disease. *Biol. Psychiatry* **74**(5), 340–347 (2013)